Reorientational Dynamics of Amide Ions in Isotypic Phases of Strontium and Calcium Amide II. Solid State NMR

J. Senker*,† and H. Jacobs

Lehrstuhl für Anorganische Chemie I, der Universität Dortmund, D-44221 Dortmund, Germany

M. Müller‡ and W. Press

Institut für Experimentelle und Angewandte Physik, der Universität Kiel, D-24098 Kiel, Germany

G. Neue

Lehrstuhl für Physikalische Chemie, der Universität Dortmund, D-44221 Dortmund, Germany

Received: November 13, 1998; In Final Form: February 23, 1999

^{2}H and ^{1}H wide-line NMR spectroscopy were used to study molecular dynamics of amide ions in a large temperature range for strontium and calcium amides. Line shape analyses resulted in two reorientational processes on very different time scales. Above 340 K ($Sr(ND_2)_2$) and 390 K ($Ca(ND_2)_2$), respectively, slow 180° reorientational jumps about the C_2 axis of the ND_2^- ions were detected. The jump rates τ^{-1} follow an Arrhenius law with activation energies of 56.8(6) kJ/mol ($Sr(ND_2)_2$), 69.2(8) kJ/mol ($Ca(ND_2)_2$), and τ_0^{-1} equal to 6(2) $\times$ 10^{12} Hz ($Sr(ND_2)_2$), 2.3(7) $\times$ 10^{13} Hz ($Ca(ND_2)_2$), respectively. The DND bond angle was determined to be 106.4(5)° and 105.7(6)° for strontium and calcium amides. Furthermore, fast rotational dynamics was observed which could be identified as strongly anisotropic, librational motion of the amide ions. This can be clearly seen from the large asymmetry parameter of the electric field gradient tensor even at low temperatures ($\eta \approx 0.2$). A simple model allows to obtain amplitudes of libration. Magnitude and temperature dependence fit well to results from recent high-resolution neutron powder diffraction investigations.[12]

Introduction

Alkali and alkaline earth metal amides are ionic compounds which show a large variety of different crystalline phases as a function of temperature.[1−3] Phase transitions between these phases as well as the phases themselves are related to dynamical processes of the amide ions.[4−13] Because of their structural simplicity they are well suited as model compounds for the detailed study of molecular dynamics. As amide ions (NH_2^-) are isoelectronic with water molecules (OH_2), an improvement of the understanding of motional processes in water-containing systems is expected, as well.

This work is the second part of an extended study of the structural and dynamical properties of calcium and strontium amides.[7,8] The first part, recently published in ref 12, deals with a detailed structure determination performed on the deuterated compounds including the positions of the deuterium atoms. Temperature-dependent X-ray scattering investigations show an abrupt change of the thermal expansion for both compounds. The corresponding transition temperatures were determined to be 295 K for $Sr(ND_2)_2$ and 370 K for $Ca(ND_2)_2$.[12] Using high-resolution neutron powder diffraction experiments, structural data were collected in a large temperature range. We extracted the probability density function (pdf) of the amide ions as well as its temperature dependence. Considering the spatial, strongly anisotropic distribution of the deuterium atoms, we suspected that librational movements with large amplitudes are involved in the nature of molecular dynamics of these compounds even at low temperatures.[12] Using the rigid-body concept for the amide ions the amplitudes of the normal librations were obtained. The temperature dependence of the wagging and twisting libration, respectively, seems to be correlated with the unusual behavior of the thermal expansion.[12]

However, whether these effects are caused by librational movements of the amide ions cannot be proved by diffraction measurements alone. In 1969, Dufourc et al.[14] published results of ^{1}H NMR investigations on both compounds. For three temperatures (110, 300, and 360 K) they analyzed the second moments M_2. Because of their temperature dependence, Dufourc et al. assumed the presence of 180° jumps about the 2-fold axis of the amide ions above 300 K. Though, they used a structure model proposed by Bouclier et al.[15] based on X-ray and infrared data which is not compatible with our neutron diffraction data.[12] Therefore, these results have to be assessed critically. To make further progress in analyzing the type and time scale of the molecular motion, we combined different analytical methods such as quasielastic (QNS) and inelastic (INS) neutron scattering as well as solid-state NMR spectroscopy in a cooperation of two groups, one in Kiel and the other in Dortmund, to investigate molecular dynamics in a large range of time scales (10^{-2} to 10^{14} Hz). The temperature was varied between 80 and 560 K for both compounds. To focus on movements of the hydrogen atoms and the amide ions, respectively, we carried out QNS and INS measurements on the protonated substances. Using the

† Present address: Experimentalphysik II, der Universität Bayreuth, D-95440 Bayreuth, Germany.

‡ Present address: European Synchrotron Radiation Facility, B. P. 156, F-38042 Grenoble Cedex 9, France.

10.1021/jp984424f CCC: $18.00
Published on Web 05/01/1999

deuterated compounds equivalent information concerning slower dynamics can be obtained with ^{2}H solid-state NMR measurements. The latter is the main aim of the present work.

Theory

In recent years ^{2}H NMR spectroscopic investigations have become an important source of information about dynamical processes in solid materials.[16] This is due to a large variety of different techniques which allow the study of fast motions (10^8−10^{12} Hz) using T_1 and T_{1Q} relaxation,[17−20] slow motions (10^3−10^8 Hz) by analyzing the line shapes of the quadrupolar spectra,[21−23] and ultra slow motions (10^{-2}−10^4 Hz) by means of selective inversion[24] or 2D exchange experiments.[25−27]

As reorientational processes presented in this paper are slow for both compounds, we concentrate on the theory of simulating the line shapes of ^{2}H spectra in the slow motion limit. As many publications dealt with its theoretical aspects in detail,[21−23,28−31] we only give a brief summary of the theory; it also serves to introduce our nomenclature.

The quadrupole moment of a deuteron interacts with the electric field gradient (EFG) tensor at the atomic site. Consequently, the resonance frequency ω is a function of the orientation of the principal axis system (PAS) of the EFG and the laboratory axis system (LAS) determined by the external magnetic field with ω_0 being the Larmor frequency: $\omega = \omega_0 + f(\alpha, \beta, \gamma)$. For a covalently bound deuterium atom, the EFG is completely dominated by the electron distribution of the σ-bond and, therefore, its PAS may be correlated with an orthonormal molecular frame, the so-called crystal axis system (CAS). The latter is defined with respect to the symmetry of the molecule and its reorientational processes, respectively.

Consider now a single deuteron whose quadrupole-coupling tensor can switch between N different sites. It is convenient to define their orientations relative to the CAS. The site frequencies ω_j thus may be calculated using irreducible second rank tensor operators for the representation of the interaction Hamiltonian. In this paper we use the conventions of Rose as delineated by Brink and Satchler[33] or Spiess.[34] Taking into account only the secular part of the quadrupolar Hamiltonian, the site frequency ω_j is thus given by

$$\omega_j = \pm\sqrt{\frac{3}{2}}\frac{e^2 qQ}{2\hbar}\sum_{n,a=-2}^{2}\rho_{2n}D^{(2)}_{na}(\Omega_j^{PC})\,D^{(2)}_{a0}(\Omega^{CL}) \quad (1)$$

Here the Eulerian transformations $\Omega = (\alpha, \beta, \gamma)$ rotate the PAS into the CAS (Ω^{PC}) and the CAS into the LAS (Ω^{CL}). In the PAS, the only nonvanishing elements of the quadrupole-coupling tensor ρ are $\rho_{20} = (3/2)^{1/2}$ and $\rho_{2\pm2} = 1/2\eta$ with η being the asymmetry parameter. Following the convention of Abragam[31] we chose the Cartesian components of the quadrupole-coupling tensor in a way that

$$|\rho_{ZZ}| \geq |\rho_{YY}| \geq |\rho_{XX}| \quad (2)$$

The spectral line shape is then obtained by solving a set of N-coupled, first-order differential equations with constant coefficients[31,32] leading to a Bloch−McConnel-type equation.

$$\frac{d\mathbf{G}}{dt} = \mathbf{G}(i\omega + \pi) \quad (3)$$

The elements of the row vector **G** are the complex transverse magnetization vectors associated with one component of the quadrupolar doublet arising from each of the orientational sites in absence of exchange. ω is a diagonal matrix including the site frequencies ω_j ($\omega_{ij} = \omega_j s_{ij}$) and π is the exchange matrix. The off-diagonal elements π_{ij} represent the jump rates from orientation i to orientation j. For reasons of microreversibility,[31] the elements π_{ij} must also fulfill the following condition which is often called detailed balance.

$$p_i\pi_{ij} = p_j\pi_{ji} \quad (4)$$

Here p_j is the a priori probability of finding the deuteron on site i. Consequently, π is a symmetric matrix only if all a priori probabilities are equal. The diagonal elements of π are always the negative sum of one row ($\sum_j \pi_{ij} = 0$).

To obtain ^{2}H-spectra, usually a solid-echo technique is used. In such an experiment the spectrometer frequency is adjusted to resonance and two 90° pulses are applied in quadrature phase which are separated by the time t_1. Just after the time t_1 following the second pulse an echo occurs which can be easily collected. The evolution of the transverse magnetization under the influence of the quadrupolar interaction may be calculated by integrating eq 3 over the complete time period t starting directly after the first pulse and including the complete echo decay. For brief and intense pulses, the effect of the second pulse on the spin system is to transform the magnetization vector $\mathbf{G}(\tau^-)$ directly before the pulse to $\mathbf{G}(\tau^+) = \mathbf{G}^*(\tau^-)$ just after the pulse.[31] Taking this effect into account and adding up the components of the transverse magnetization vectors for each site, we get

$$K(t,t_1) = \mathbf{G}^*(0)\exp((-i\omega + \pi)(t - t_1))\exp((i\omega + \pi)t_1)\mathbf{1} \text{ mit } t > t_1 \quad (5)$$

It is worth noting that $K(t,0) = G^*(t)$, $K(\tau,\tau) = \mathbf{G}(\tau)$, and $K(t,\tau)$ becomes $G^*(t\text{-}2\tau)$ in the rigid limit ($\pi \rightarrow 0$) where the solid-echo decay is identical to the FID (free induction decay) except for a time shift of 2τ.

Summing up, the echo decay over all possible orientations of small crystals in a powdered sample and Fourier transforming from the top of the echo with respect to t yields the line shape of the deuterium echo spectra. For technical reasons due to finite pulse length and filter delays, normally the top of the echo is moved to slightly longer times t. In practice it is also necessary to correct the resulting spectrum with terms which account for uneven excitation by finite rf pulses,[35] for contributions from the virtual FID,[36,37] and for contributions of dipolar coupling to other nuclei in the neighborhood of the corresponding deuteron (see following section).

Motionally narrowed spectra in the presence of fast motion simply can be calculated by averaging the frequencies of each involved motional site achieved from eq 1.

$$\bar{\omega} = \sum_j p_j\,\omega_j \quad (6)$$

Afterward, a powder average has to be performed. However, it is often useful to introduce an effective quadrupole-coupling tensor $\mathbf{Q}^{eff}$ to characterize the motionally narrowed spectra using a Cartesian representation. Its elements can easily be calculated from the tensor **Q** of a rigid ND bond in its principal axes representation by using

$$\mathbf{Q}^{eff}_{kl} = \sum_j p_j\,(\mathbf{R}(\Omega_j)\mathbf{Q}\,\mathbf{R}(\Omega_j)^{-1})_{kl} \quad (7)$$

where **R** is the Cartesian Eulerian matrix (see also ref 34 Appendix C) for the transformation of the quadrupole-coupling

tensor into the crystal axes system and $\Omega_j = (\alpha_j, \beta_j, \gamma_j)$ is the angle triple of a deuteron on site j. Its principal axis values were obtained by solving the eigenvalue equation.

Experimental Details

Preparation and characterization of the samples investigated here are described in detail in ref 12.

^{2}H quadrupole powder spectra were obtained with a conventional pulse spectrometer MSL 400 P (Bruker Physics, Karlsruhe) at a resonance frequency of 61.4 MHz. For temperatures below room temperature, a special low-temperature ^{2}H probe (HP.LT.BB.060 SOL 5, Bruker Karlsruhe, Q = 60) was used. It was placed in a cryostat K 1500 (Oxford Instruments) which was cooled with liquid nitrogen. For temperatures above room temperature, we used a cross-polarization probe (HP.WB.73A SOL 5 CP.BB, Bruker Karlsruhe, Q = 136) and the ^{1}H powder spectra were measured at a resonance frequency of 400 MHz with a ^{1}H probe (HP.WB.73AFF SOL 5, Bruker Karlsruhe, Q = 80) especially designed for short dead times. Both probes could be heated and cooled, respectively, in a temperature range between 150 and 570 K with a constant gas flow of dry nitrogen. The temperature stability was better than 0.3 K in the whole temperature range, and reported temperatures were believed accurate within ±1 K. All probes mentioned above are equipped with a solenoid coil with a diameter of 5 mm and a length of 20 mm. We filled quartz glass tubes of suitable dimensions with pulverized samples in a self-made glovebox[38] and sealed them off immediately after locking them out of the box.

Most ^{2}H-spectra were measured applying a standard solid-echo pulse sequence[39] (90_x-t_1-90_y-ACQ). To suppress the most frequent artifacts we cycled the phase of the second pulse ($\phi \pm 90°$) with respect to the first and additionally alternated the phase of the first pulse between 0 and 180°, leading to a four-step phase cycle. Typical 90° pulse lengths were in the range of 3 μs and the interpulse spacing t_1 mostly was fixed to 20 μs. For some temperatures, t_1 was also varied as an additional check of the model of motion. In connection with this we had to take care of the anisotropic effect of ^{14}N spin-lattice relaxation for the echo dephasing, leading to a significant contribution to the transverse relaxation rates of the deuterons for long evolution periods.[40] To avoid an influence on our analysis, we limited t_1 to less than 50 μs.

Especially in the intermediate exchange region, the spin−spin relaxation time T_2 becomes very short because of an efficient exchange-induced dephasing. It cannot be refocused by the second pulse of the solid echo and, therefore, these echo spectra are strongly attenuated. In fact, the intensity was so small that their shape was distorted by acoustic ringing which normally can be neglected at such a high resonance frequency of 61.4 MHz. Being aware of the fact that acoustic ringing of both pulses cannot simply be cycled out, we introduced a 180° pulse just before every second solid-echo sequence making use of the fact that the signal of the acoustic ringing is correlated with the pulse phases. By subtracting both acquisitions, acoustic ringing could be suppressed while the echo adds up (180_x-t_2-90_x-t_1-90_y-ACQ_{-x}-90_x-t_1-90_y-ACQ_x). Here, t_2 must be longer than the dephasing time of the ringing and much smaller than T_1. We choose t_2 of the order of the acquisition time of ≈ 1 ms, whereas the spin lattice relaxation time is in the range of tens of seconds for temperatures where this sequence has to be applied. To achieve an inversion as complete and distortionless as possible, we designed the 180° pulse by a composite pulse. The best results were obtained by using three back-to-back 90° pulses with switching the phase of the middle pulse by 90° (90_ϕ-$90_{(\phi\pm90)}90_\phi$).[41] The 90° pulses again were replaced by a Levitt−Suter−Ernst triplet[42] ($135_\phi 90_{(\phi+180)} 45_\phi$). ϕ was cycled with respect to the before mentioned phase cycle of the solid-echo sequence, leading to a 16-step phase cycle.

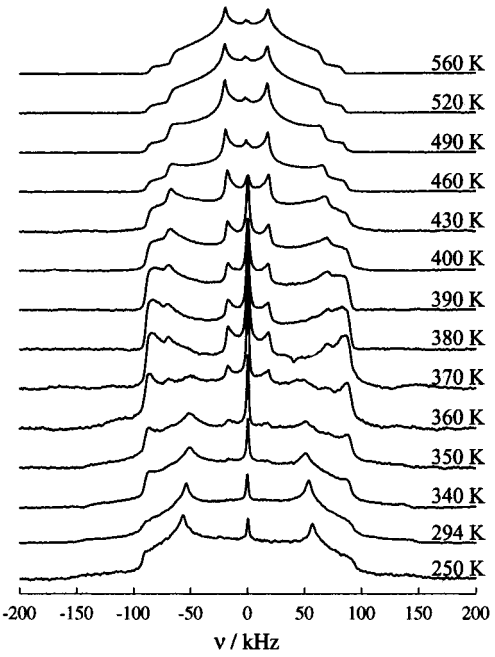

Figure 1. Typical ^{2}H-spectra of $Sr(ND_2)_2$. The spectra were recorded with a constant interpulse spacing t_1 of 20 μs. Other acquisition parameters are given in the text. Each spectrum was normalized to unit intensity. The additional narrow Lorentzian line in some spectra is caused by mobile deuterated ammonia which was adsorbed on the material surface during sample preparation. The spectra are not symmetrized.

To ensure the correct finding of the echo maximum which is essentially important for an accurate determination of jump rates from the spectra, always a dwell time of 0.1 μs was used.

The ^{1}H NMR experiments were carried out with a simple one-pulse acquisition in a cycle observation. The 90° pulse was of the order of 2.5 μs and dead times were shorter than 2 μs.

Line shape simulations for ^{2}H spectra in the intermediate exchange region were performed with some routines of the program MXQET,[22] which are based on eqs 1−5. Besides a high flexibility in realizing different models of motion, these routines consider the most frequent artifacts arising from finite pulse power. Additionally, dipolar broadening was introduced in the simulation by convoluting the calculated spectra with a Gaussian and a Lorentzian line, respectively. Correcting for small asymmetries of all observed ^{2}H spectra, which is clearly associated with the resonance shape of the used commercial probes, we symmetrized the observed spectra before performing the fit. To follow the temperature dependence of the molecular dynamics in detail and to get precise information about the jump rates as a function of temperature we coupled this program to a least-squares algorithm.

Results and Discussion

Wide-line ^{2}H NMR spectra were measured in a temperature range of 200 to 560 K for both compounds. Apart from a slight shift to higher temperatures for $Ca(ND_2)_2$, the spectra as well as their temperature dependence are similar (see Figures 1 and 2), implying an analogous dynamical behavior of the amide ions. For temperatures less than 340 K ($Sr(ND_2)_2$) and 390 K ($Ca(ND_2)_2$), respectively, the ^{2}H spectra consist of broad powder patterns typical for nonaxially symmetric interaction tensors.

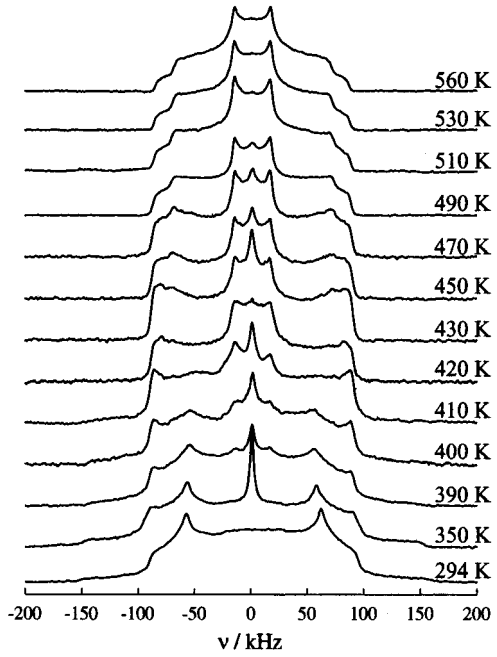

Figure 2. Typical ^{2}H-spectra of $Ca(ND_2)_2$. For further information refer to the caption of Figure 1.

Estimated quadrupole-coupling constants (QCC) are of the order of 200 kHz, and the asymmetry parameters η are roughly 0.25. With increasing temperature the line shapes change resulting in a partially motionally narrowed powder pattern at high temperatures (>520/560 K $Sr(ND_2)_2/Ca(ND_2)_2$). Its spectral width is nearly 2/3 compared with the spectral width of the low-temperature spectra. Especially in the temperature range 350−390 K/410−450 K ($Sr(ND_2)_2/Ca(ND_2)_2$), the spectral intensities are strongly attenuated.

Just from a first look at the experimental data, some conclusions on the reorientational dynamics of the amide ions can be drawn. The strong line shape changes together with the strong attenuation, typical for a slow exchange, show the presence of a slow dynamical process above room temperature. The frequency of the *y*-axis of the PAS of the low-temperature quadrupole-coupling tensor (shoulders of the spectra; $\approx \pm 100$ kHz) is roughly the same as the frequency of the *z*-principal axis of the motionally narrowed interaction tensor system (feet of the high-temperature spectra). This indicates that the *y*-principal axis of the low-temperature tensor remains unchanged with respect to the aforementioned slow reorientational motion. Therefore, our line shape analyses only have to consider models for the amide ion reorientations for which all sites involved are facing one plane which also must be perpendicular to the *y*-axis. Furthermore, possible models for the slow dynamical process also must correspond to the motionally narrowed, effective quadrupole-coupling tensor calculated from the motionally narrowed spectra in the high-temperature regime (T > 500 K), yielding values of the order of 120 kHz for QCC^{eff} and 0.6 for η^{eff}.

Another striking point is the large asymmetry parameter ($\eta \approx 0.25$) needed to describe the low-temperature spectra. The quadrupole-coupling tensor of a nitrogen bound deuterium atom in a rigid lattice mostly can be dealt with as axially symmetric because of the dominant influence of the covalent σ-bond to the electric field gradient. Usually only small values up to 0.05 for η have to be considered. Furthermore, the observed QCC $\approx$ 200 kHz in the low-temperature regime is too small for a deuterium atom in a rigid amide group proving the existence

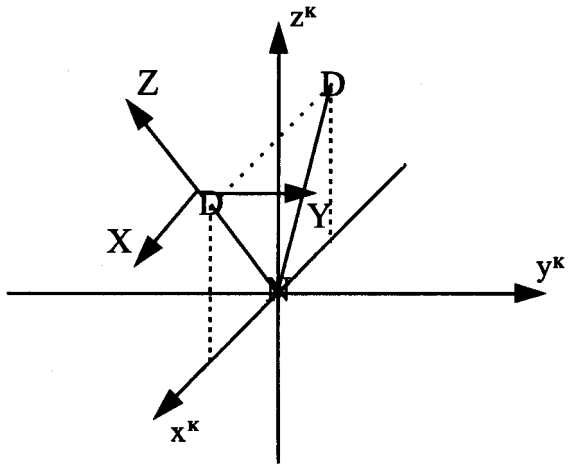

Figure 3. Orientation of the PAS of the effective quadrupole coupling tensor (X, Y, Z) with respect to the CAS of an amide ion (x^K, y^K, z^K).

of a fast, spatially anisotropic rotational motion even at low temperatures for both compounds which reduces the static values. A theoretical study[46] on deuterated ammonia obtained values between 250 and 280 kHz for a static QCC dependent on the chosen basis set. Reported values[43−45] which were experimentally determined are in the range of 220−240 kHz. With respect to the theoretically calculated values, the latter are probably reduced by some fast motion as well. Extremely long spin-lattice relaxation times (T_1 > 150 s) in this regime also indicate that for this process the dynamics is not relaxational but librational in nature. This corroborates the results of recently reported neutron diffraction investigations on both materials[12] obtaining large anisotropic amide librations at low temperatures.

The amide ion librations are fast compared to the time scale of ^{2}H NMR ($\tau^{-1} \ll \Delta$) and, therefore, we will refer to their influence on the spectra only in the form of a reduced effective quadrupole-coupling tensor as starting tensor for our line shape analyses below. As the libration amplitudes will turn out to be temperature-dependent (see below), the resulting effective quadrupole-coupling tensor will be a function of temperature as well. This treatment also contains the advantage of time saving line shape simulations because of a significant reduction of necessary reorientational sites for our models of motion. It is known from ref 12 that the rocking libration of the amide group (vibration in the molecular plane of the amide ions) is much larger than any librational motion perpendicular to the amide plane (wagging and twisting). Consider an axially symmetric quadrupolar-coupling tensor for a rigid deuterium atom with its *z*-principal axis aligned with the ND bond. The other two principal axes are perpendicular to the *z*-axis and have no preferred orientation. However, the librational motion reduces elements of the rigid quadrupolar coupling tensor perpendicular to the amide plane less than other elements, introducing non-axiallity to the effective quadrupolar coupling tensor. Considering eq 2 and the symmetry of the amide librations, the *Z*-principal axis of the effective quadrupolar coupling tensor still will be aligned with the ND bond and the *Y*-principal axis turns out to be perpendicular to the amide plane. The *X*-principal axis is perpendicular to both and faces the amide plane (see Figure 3).

Taking into account the symmetry of the amide ions, we chose the crystal axes system (x^K, y^K, z^K) aligned with the principal axes system of the moment of inertia with its z^K-axis parallel to the 2-fold axis. Thus, the x^K-axis is perpendicular to the C_2 axis and faces the amide plane (see Figure 3). To simplify the following calculations we used the nitrogen position as mole-

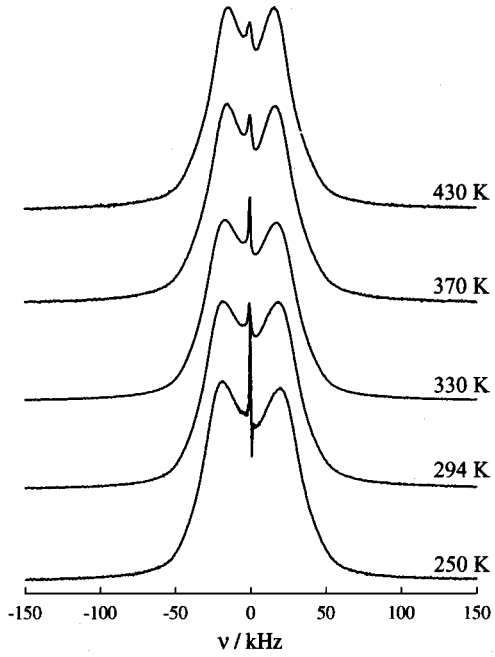

Figure 4. Typical ^{1}H NMR spectra of $Sr(NH_2)_2$. The spectra were recorded with a one pulse aquisition and normalized to unit intensity.

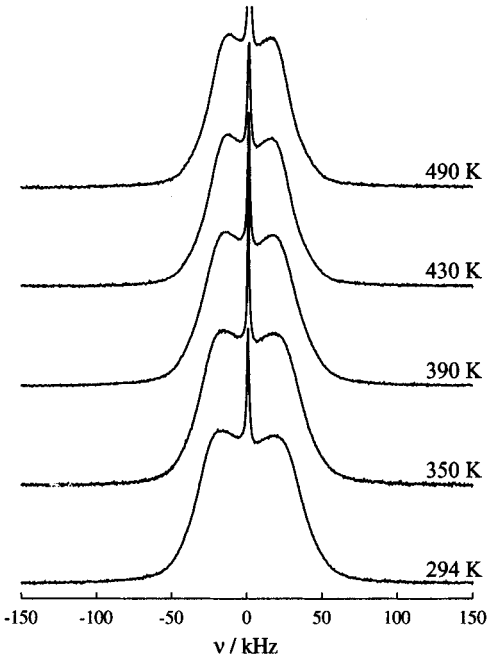

Figure 5. Typical ^{1}H NMR spectra of $Ca(NH_2)_2$.

cular center instead of the center of mass of the amide ions, knowing well that the arising error will be small (<1%). The above-mentioned conditions for the motional models can be met by assuming reorientational jumps about one of the three principal axes of the moment of inertia of the amide ions. The angle between the rotation axis and the *z*-axis of the librationally narrowed coupling tensor has to be chosen to be roughly 37° or the complementary angle 90° − 37° = 53° in the case of two site jump models to fit both low- and high-temperature spectra. If more than two sites are considered, the angle of maximum rotational displacement must be of the same order or even larger as for two site models.

Taking into account the spatial distribution of the probability density function (pdf) and its temperature dependence (see Figure 8 in ref 12) probed with neutron diffraction experiments the number of possible models can be reduced considerably. Because of the above-mentioned facts, the need of large rotational displacement reorientations about the x^K-axis can be excluded. For the same reason, reorientations about the 2-fold axis with the exception of 180° rotational jumps can be eliminated as well as 180° reorientations about the y^K-axis. In contrast, 180° jumps about the C_2 axis and torsional motions of the amide groups about the y^K-axis with two or more sites are compatible with the line shape changes of the ^{2}H NMR spectra and the spatial distribution of the pdf.

Further models can be excluded considering the temperature dependence of the wide-line ^{1}H NMR spectra measured within the critical temperature range (250−500 K) for both compounds (see Figures 4 and 5). The proton−proton distance in one amide group is roughly 1.54 Å, i.e., markedly smaller than the next neighbors' proton−proton distances which are larger than 2.05 Å.[8,12] Thus the strength of the dipolar coupling to surrounding protons is at least by a factor of 3 smaller than the coupling between the two protons within one group. This is also valid for the strength of the heteronuclear dipolar coupling of the nitrogen atom and the hydrogen atoms of one amide group. Therefore, the proton wide-line spectra can be interpreted according to a dipolar coupled pair of spins $I = {}^1/_2$ with an axially symmetric interaction tensor. But because of the interactions discussed above, the resulting Pake spectrum is strongly broadened. Reorientational motion of a protonated amide group consequently can be described in complete analogy with the case of deuterons.[32,34] The new aspect as compared with the latter is the different orientation of the principal axis system (*X, Y, Z*) of the dipolar interaction tensor with respect to the principal axis system (x^K, y^K, z^K) of the moment of inertia of the amide ions. Whereas the *Z*-axis of the quadrupolar coupling tensor is aligned with the ND bond in the case of deuterons (see Figure 3), the *Z*-axis of the dipolar coupling tensor is aligned with the internuclear axis between both protons in one amide group in the case of protons.

For the 180° reorientational jump about the C_2-axis, the effective dipolar coupling tensor, therefore, will not be reduced, so the shape of ^{1}H-spectra should not change as a function of temperature. On the contrary, the effective dipolar coupling tensor partially will be averaged for torsional motion of the amide ions within the amide plane and the width of the ^{1}H-spectra should markedly reduce at higher temperatures. Indeed, in this case the ^{1}H-spectra should reveal analogous line shape changes as observed for the ^{2}H-spectra in the intermediate exchange region. The observed ^{1}H-spectra (see Figures 4 and 5) exhibit no qualitative change of the line shapes except from a slight decrease of the spectral width with increasing temperature caused by the amide librations (for details see below). Thus, the slow dynamical process can be interpreted as a 180° reorientational jump of the amide ions about their C_2 axis.

Qualitatively, we were able to favor one particular model for the slow motional process of the amide ions. To underline our argumentation further we performed line shape simulations for the ^{2}H-spectra as well. Parameters used for these simulations are listed in Table 1. Both two-site models, the 180° jump about the C_2 axis and the two-site torsional motion about the y^K-axis yield identical spectra as a function of the static quadrupole-coupling tensor and the jump rate which is due to symmetry arguments for trigonometric functions. The simulated spectra for both models are depicted in Figure 6a. Furthermore, we probed jump processes containing three and four sites and considered nearest neighbor jumps as well as all-site exchange

TABLE 1: Model Parameter for the Deuterium NMR Line Shape Simulations[a]

	jump models			restricted diffusion	
				box pot.	harmonic pot.
sites	2	3	4	17	7
orientation ($\alpha_i,\beta_i,\gamma_i$) (deg)	(0,ϵ,0)	(0,47,0)	(0,51,0)	(0,64,0)	(0,84,0)
	(0,ϵ,180)	(0,0,0)	(0,17,0)	(0,56,0)	(0,56,0)
		(0,47,180)	(0,17,180)	⋮	⋮
	$\epsilon = 37$ or 53		(0,51,180)	⋮	⋮
				(0,56,180)	(0,56,180)
				(0,64,180)	(0,84,180)
a priori probabilities p_i	$p_i = 0.5$	$p_i = 1/3$	$p_i = 0.25$	$p_i = 1/17$	$p_1 = p_7 = 0.0292$
					$p_2 = p_6 = 0.1461$
					$p_3 = p_5 = 0.2087$
					$p_6 = 0.2320$
exchange model	nearest neighbor and all site exchange			only nearest neighbors	

[a] Only jump angles were considered which are compatible with the distribution of the aforementioned pdf. The Eulerian angles given here are defined with respect to the CAS given in the text (see also Figure 3). For all models we used a QCC of 200 kHz and $\eta = 0.27$ for a rigid deuteron. The evolution time t_1 was varied between 10 μs and 50 μs, the 90° pulse length was chosen to be 2.5 μs, and a Gaussian broadening of 1 kHz was used.

models. These four models also reveal similar spectra which are shown in Figure 6b.

Because of the pdf, which is strongly smeared out within the amide plane,[12] rotational diffusional motion of the amide ions within the amide plane seems to be possible as well. Therefore, we tested for restricted diffusion in a box potential and in a flat harmonic potential, which was introduced into our simulations by assigning each site an individual a priori probability (see Table 1). For the latter we refer to ref 12 where a potential for small angle rotations of an amide ion in its molecular plane was calculated on the basis of a purely electrostatic model. Greenfield et al.[22] showed that diffusional models can be approximated by jump models if only small angle jumps are considered for the elementary process. We tried jump angles between 5° and 20° which correspond to 7 and 17 sites for the diffusion in a box potential. The resulting spectra are nearly the same. This justifies the building up of the diffusion model in a curved potential with a minimum of sites to reduce the large computation times due to time-consuming diagonalization procedures for the exchange matrix π. Therefore, only seven sites were included. The corresponding ^{2}H NMR spectra are presented in Figures 6c and 6d.

It is obvious that only the simulated deuterium spectra for both possible two-site jump models fit to the experimentally derived data. This is valid for line shape changes as a function of the jump rate (see Figure 3a) as well as for the dependence of the deuterium echo spectra on the evolution time t_1 which is displayed exemplarily in Figure 7 for $Sr(ND_2)_2$ at 400 K. It is not possible to decide between these only on the basis of ^{2}H NMR experiments. However, a 180° reorientational jump about the 2-fold axis of the amide ions is the only model which is compatible with the ^{2}H NMR, ^{1}H NMR, and neutron diffraction[12] data.

To determine the jump rates as a function of temperature, we fitted the ^{2}H-spectra of both compounds using the program MXQET[22] coupled to a least-squares program (see previous section). At lower temperatures where the jump rates are of the order of 10^4 Hz, additionally, the angle of the *Z*-axis of the "static" coupling tensor with the rotation axis (C_2 axis) could be determined, which corresponds to half of the DND bond angle. The narrow resonance ($\Delta\omega \approx 1$ kHz) roughly at ω_0 caused by absorbed deuterated ammonia (due to sample preparation[8,12]) was considered by introducing a Lorentzian line into our fit routine. In the case of $Ca(ND_2)_2$, an additional Gaussian resonance ($\Delta\omega \approx 60$ kHz) had to be taken into account to fit the spectra at higher temperatures. Its intensity is $\leq 15\%$ of the whole spectrum depending on temperature and pretreatment of the samples (see Figure 8). This resonance is due to the beginning decomposition of calcium amide to calcium imide and ammonia which was shown by vacuum decomposition experiments with a Hüttig Tensieudiometer[47] and by thermogravimetric measurements where a loss of weight was obtained. The existence of Ca(ND) in our samples was proved by X-ray scattering and IR and Ra spectroscopic investigations. A detailed study of this effect is given in ref 8.

All observed ^{2}H-spectra of both compounds could be well fitted. Some profile fits are displayed in Figure 9, and relevant refinement parameters are listed in Tables2 and 3. From the spectra at 340−360 K for $Sr(ND_2)_2$ and 380−410 K for $Ca(ND_2)_2$, the DND bond angle was determined. Within the accuracy of the measurements, the average values for both compounds are identical and are listed in Table 4.

The achieved jump rates follow an Arrhenius law (see Figure 10) for both compounds, indicating that the 180° reorientational jump can be understood as a thermally activated single particle motion. This is also indicated by the agreement of the attempt frequencies and the frequencies of the normal librations of the amide ions (see Table 4). The librational frequencies were obtained by means of Raman scattering (for experimental details see ref 12). On the basis of a factor group analysis (see Figure 11) carried out with the structural model developed from high-resolution neutron scattering experiments[12] using the correlation method,[48] we were able to assign the normal librations of the amide ions definitely. All three normal libration modes (rocking R_r; wagging R_γ; twisting R_t) are absorptive in the Raman spectrum and show no splitting under the influence of the crystal symmetry. Taking advantage of this fact and the characteristic isotopic shift of the frequencies of the librational modes for the protonated and the deuterated compounds ($\nu_{NH_2^-}/\nu_{ND_2^-} = 1.36$), we were able to separate the normal librations from the lattice modes.

The most striking point considering the refinement parameters of the line shape analyses of the ^{2}H NMR spectra is the strong temperature dependence of the "static" quadrupole-coupling constant QCC and the "static" asymmetry parameter η derived as fit parameter (see Tables 2 and 3). As aforementioned, it must be caused by a fast, spatially anisotropic, dynamical process of the amide ions. It was identified as librational motion by neutron scattering.[12] To describe the thermal behavior of the amide librations more quantitatively, we chose values for a quadrupole-coupling tensor of a deuteron belonging to a static ND bond and we needed a pdf for the librations to calculate

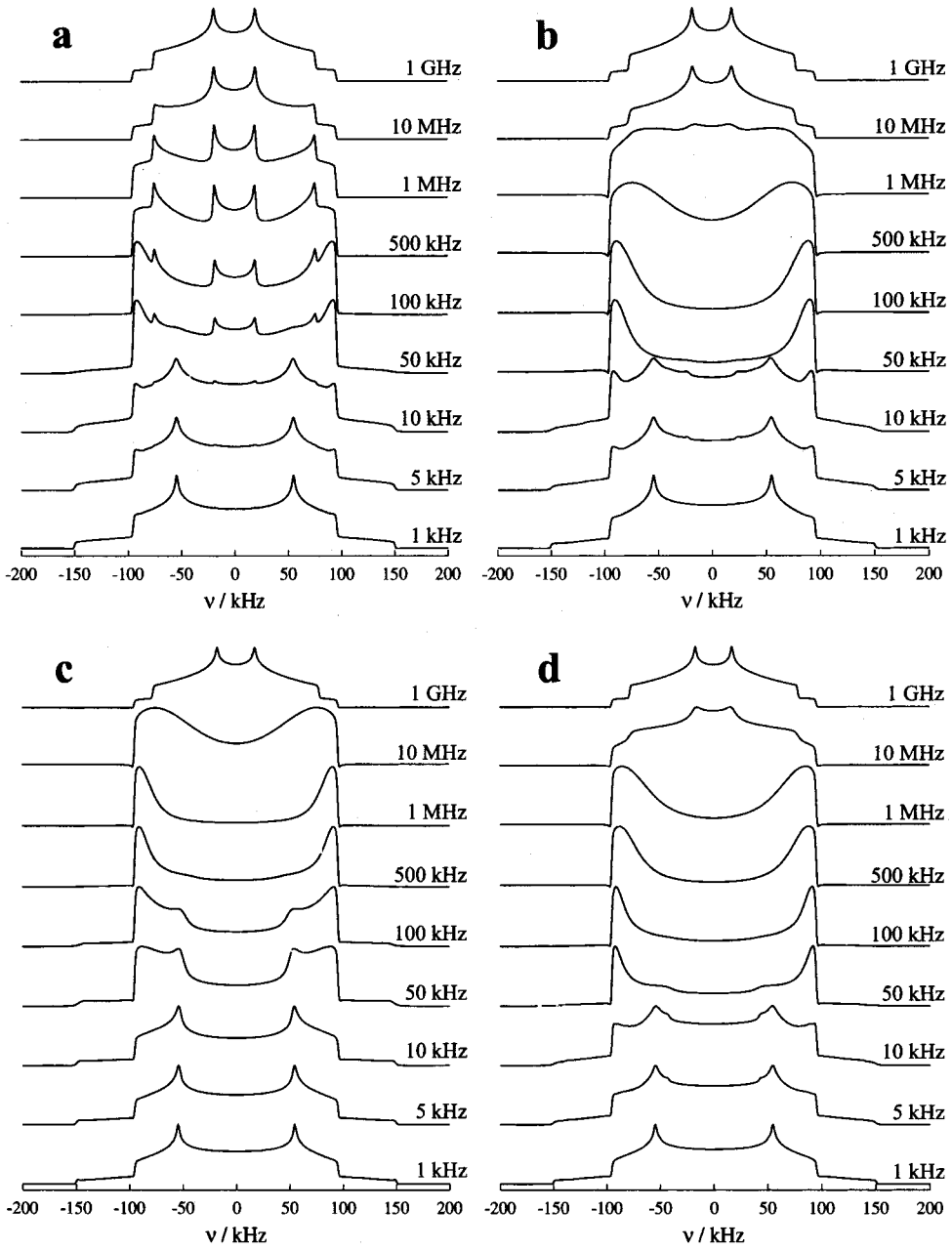

Figure 6. Simulated ^{2}H powder spectra with variable jump rates for 180° reorientational jumps (a), three and four site jumps within the amide plane (b), and restricted diffusion in a box (c) and a harmonic potential (d). Model-specific parameters are listed in Table 1. The evolution time t_1 is 20 μs for all displayed spectra.

the effective quadrupole-coupling tensor based on eq 7. Due to the fact that only two independent parameters could be determined by measuring ^{2}H NMR spectra in the case of fast motion, we are forced to parameterize the librational motion which is a superposition of three normal modes. The rocking libration causes a rotation of the deuterium atoms within the {1 0 0} planes, whereas the wagging and the twisting modes move deuterium atoms out of the these planes. The pdf of the wagging and the twisting modes are very similar, especially for considerably small amplitudes (<40°). Therefore, it is sufficient for our calculations to take into account only one of both. To stay close to the analyses of the neutron scattering experiments[12] we used the wagging mode and ignored the twisting vibration.

For both remaining normal librations, the wagging and the twisting mode, we considered two sites for each of them, characterizing the turning points of the librational movement to approximate the pdf. So our model contains four sites distributed on a sphere with a radius equal to the length of the ND bond and two independent parameters. The librational motion is fast on the time scale of the NMR and, thus, only geometric aspects of the dynamical process influence the shape of the 1D spectra. This means that several different models for the pdf of the normal librations could be used for calculating the libration amplitudes, and the NMR data do not favor of one of them. However, it was shown[8] that mostly the libration amplitudes vary probing different models, whereas the temperature dependence and the ratio between the out-of- and in-plane librations remain nearly unchanged. The model used for the present work is the most simple model and is, therefore, easy to handle. It always yields the smallest amplitudes for a given pair of QCC_{eff} and η_{eff} and has, therefore, to be understood as a lower limit of the amplitudes. The static QCC was set to 250 kHz, and the static η is equal to zero according to the symmetry of the covalent ND bond. In literature,[43−46] values

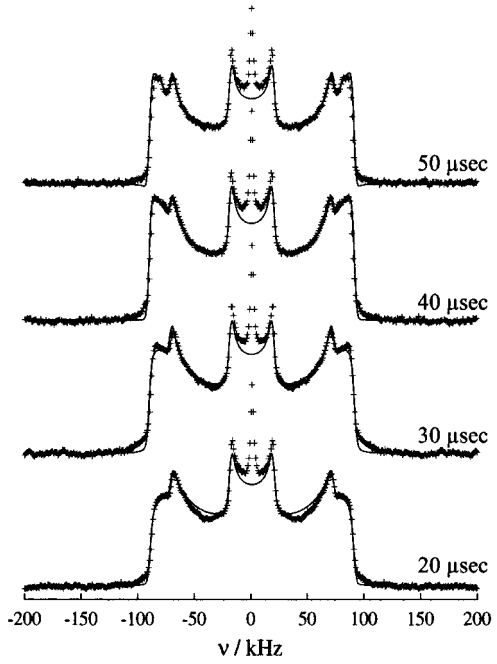

Figure 7. Profile fits for ^{2}H-spectra of $Sr(ND_2)_2$ at 400 K with variable evolution time t_1. For QCC and η, the jump rate and the DND bond angle, the values listed in Table 2 were used. The experimental spectra (+) are symmetrized.

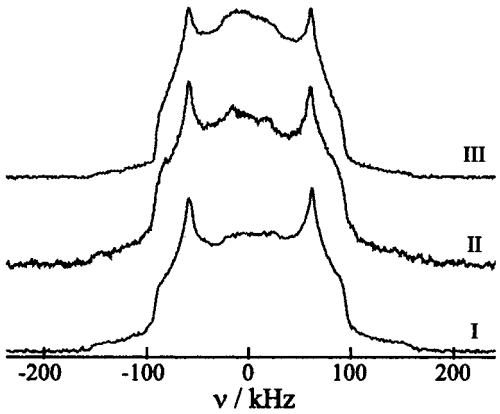

Figure 8. ^{2}H-spectra of $Ca(ND_2)_2$ using samples with different conditions of preparation. All spectra were collected at room temperature. Sample I was degassed in dynamical vacuum for 2 h at room temperature. Sample II was heated to 470 K for 2 days in a sealed glass container, and sample III was degassed in dynamical vacuum at 420 K for 5 h. The molar amount of Ca(ND) which has been formed during the sample treatment is 3% for sample I, 6% for sample II, and 19% for sample III. For further details see ref 8.

for a static QCC were found to be in the range of 220−280 kHz. Therefore, the choice of QCC is relatively unsure and we used the smallest value for which physically proper libration amplitudes could be achieved. Smaller values of QCC result in negative amplitudes for the out-of-plane vibrations.

Thus, the absolute values for the libration amplitudes calculated from the NMR data have to be checked with an independent method which is not necessary for their temperature dependence. The libration amplitudes derived are listed in Tables 2 and 3 and are depicted in Figure 12 together with those obtained from the neutron scattering results. Both methods show the same trend for the amplitudes. Even at low temperatures the amplitude of the rocking libration is large and increases only slightly with rising temperature. In contrast, the amplitude of the wagging libration is small at low temperatures but exhibits a strong increase at 304 K for $Sr(ND_2)_2$ and 368 K for

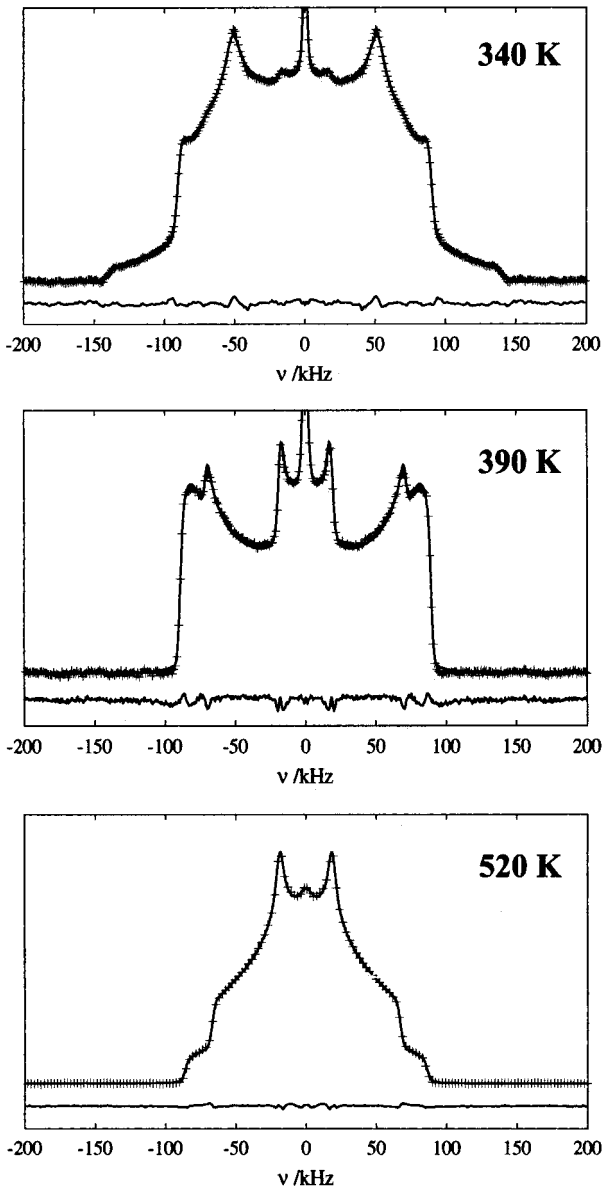

Figure 9. Profile fits for $Sr(ND_2)_2$ at various temperatures (+: experimental data; solid line: simulation). The lines displayed below the spectra are the difference curves ($I_{obs} - I_{calc}$). The fit parameters are shown in Table 2. The experimentally derived spectra again are symmetrized.

$Ca(ND_2)_2$, respectively (see Figure 12). Because of the higher accuracy, this effect is more pronounced for the NMR data.

Conclusions

Two different rotational processes of the amide ions on different time scales were observed for strontium and calcium amides. The first is a slow 180° reorientational jump of the amide ions about their 2-fold axis. This was proven by means of ^{2}H and ^{1}H solid-state NMR investigations as well as by considering the shape of the pdf of the amide ions.[12] From ^{2}H NMR line shape analyses we determined the DND bond angle, the static quadrupole-coupling tensor, and the jump rate as a function of temperature. The jump rates follow an Arrhenius law for both compounds with activation energies of 56.8(6) kJ/mol ($Sr(ND_2)_2$) and 69.2(8) kJ/mol ($Ca(ND_2)_2$), respectively. The attempt frequencies are of the same order as the frequencies of the normal librations of the amide ions obtained by Raman scattering experiments. At this point the question arises whether

TABLE 2: Relevant Refinement Parameters Obtained in Profile Fits of the ^{2}H NMR Data of $Sr(ND_2)_2$ and Estimated Libration Amplitudes[a]

T (K)	QCC (kHz)	η	ϵ (deg)	κ (kHz)	Gb (kHz)	α (deg)	β (deg)
200	204.1(4)	0.220(2)			3.0(2)	0.0(4)	19.9(4)
250	201.9(3)	0.243(1)			3.2(1)	0.0(4)	20.8(4)
294	197.0(2)	0.271(1)			3.6(1)	2.5(4)	22.0(4)
340	189.9(2)	0.273(1)	53.20(8)	14.3(1)	2.8(1)	9.1(4)	23.3(4)
350	190.2(3)	0.282(2)	53.15(7)	20.2(2)	3.2(1)	9.5(4)	23.6(4)
360	186.1(3)	0.314(2)	53.26(9)	34.5(4)	3.1(1)	9.9(4)	24.3(4)
370	187.9(4)	0.295(4)		78(1)	3.5(1)	10.2(4)	24.1(4)
380	185.0(2)	0.294(2)		89(1)	2.2(1)	9.7(4)	24.9(4)
390	183.9(2)	0.299(2)		122(3)	2.0(2)	9.9(4)	25.1(4)
400	184.1(2)	0.309(2)		234(6)	2.4(2)	11.3(4)	25.6(4)
430	179.7(3)	0.314(3)		765(10)	2.1(1)	13.1(4)	27.1(4)
460	177.6(3)	0.323(2)		2710(90)	1.6(1)	14.0(4)	28.5(4)
490	174.3(2)	0.335(3)		5590(110)	1.6(1)	14.4(4)	28.9(4)
520	171.3(3)	0.333(2)			2.0(1)	14.8(4)	29.0(4)
560	165.4(4)	0.355(3)			2.3(1)	16.0(4)	30.5(4)

[a] QCC is the coupling constant and η is the asymmetry parameter of the quadrupole-coupling tensor. 2ϵ denotes the DND bond angle and κ characterizes the jump rate of the 180° reorientational jump of the amide ions about their 2-fold axis. Gb denotes the Gaussian broadening for the simulated spectra. α and β are the amplitudes of the out-of-plane (α) and the in-plane (β) librational motions of the amide ions. Both were calculated using a model described in the text.

TABLE 3: Relevant Refinement Parameters Obtained in Profile Fits of the ^{2}H NMR Data of $Ca(ND_2)_2$ and Estimated Libration Amplitudes[a]

T (K)	QCC (kHz)	η	$\epsilon/2$ (deg)	κ (kHz)	Gb (kHz)	α (deg)	β (deg)
250	206.8(4)	0.201(3)			5.5(1)	4.3(6)	19.7(6)
294	203.9(2)	0.219(1)			3.7(1)	4.0(6)	20.3(6)
350	200.6(4)	0.237(1)			4.7(1)	4.5(6)	21.1(6)
380	194.3(3)	0.242(2)			4.4(1)	9.5(6)	21.8(6)
390	194.5(3)	0.243(2)	52.7(1)	14.1(2)	4.2(1)	9.5(6)	21.9(6)
400	193.7(3)	0.244(1)	53.0(2)	22.2(4)	3.4(2)	10.0(6)	22.0(6)
410	192.7(2)	0.246(2)	52.9(1)	35.7(5)	3.6(2)	10.4(6)	22.2(6)
420	189.6(3)	0.258(1)		59.9(10)	3.2(1)	11.2(6)	22.7(6)
430	188.2(4)	0.254(3)		85.2(30)	3.2(1)	12.4(6)	22.8(6)
450	185.2(5)	0.266(3)		220(10)	2.6(1)	13.1(6)	23.4(6)
470	183.1(4)	0.271(2)		503(40)	2.3(1)	13.7(6)	23.7(6)
490	182.5(4)	0.271(2)		935(80)	2.3(1)	14.1(6)	23.8(6)
510	182.5(4)	0.271(1)		2127(200)	2.2(1)	14.1(6)	23.8(6)
530	177.3(3)	0.294(1)			2.2(1)	15.0(6)	24.7(6)
560	176.4(3)	0.292(1)			3.0(1)	15.5(6)	24.7(6)

[a] For a detailed description of the parameters see Table 2.

TABLE 4: Fit Parameters of the Arrhenius Law and Librational Frequencies Derived from Raman Scattering Experiments

	bond angle (deg)	E_A (kJ/mol)	τ_0 (THz)	librations (THz)
$Sr(ND_2)_2$	106.4(5)	56.8(6)	6.4(20)	11.8 12.7 17.3
$Ca(ND_2)_2$	105.7(6)	69.2(8)	24.1(70)	12.0 13.4 17.0

the jump process contributes to the anomalous expansion at transition temperatures of 295 K for $Sr(ND_2)_2$ and 370 K for $Ca(ND_2)_2$,[12] which is known from X-ray diffraction. The Arrhenius-like temperature dependence of the jump rates and the order of the attempt frequencies indicate that the 180° reorientational jump is a thermally activated single particle motion. In particular, the jump rates of the 180° jump at the transition temperature are 1.1 kHz ($Sr(ND_2)_2$) and 3.6 kHz ($Ca(ND_2)_2$) extrapolated from the Arrhenius behavior of the jump rates. These rates are very slow compared to frequencies of lattice modes usually found to be in a THz range. Considering a theoretical approach of Schotte et al.,[51,52] a relaxational single particle motion only couples with lattice modes if both jump rates and frequencies of the lattice modes are of the same order. Consequently, it is highly improbable that the 180° reorientational process is involved in the anomalous thermal expansion of both compounds.

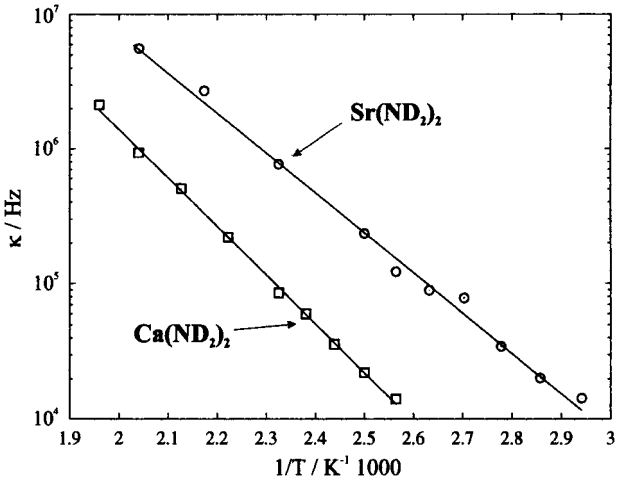

Figure 10. Arrhenius plot of the jump rates κ of the 180° reorientational jump of the amide ions about their 2-fold axis for both compounds.

The DND bond angles of the amide ions determined from the line shape analyses (see Table 4) agree well with the value of 104(2)° derived from neutron scattering experiments for both compounds.[12] The bond angle for $Ca(ND_2)_2$ is slightly smaller

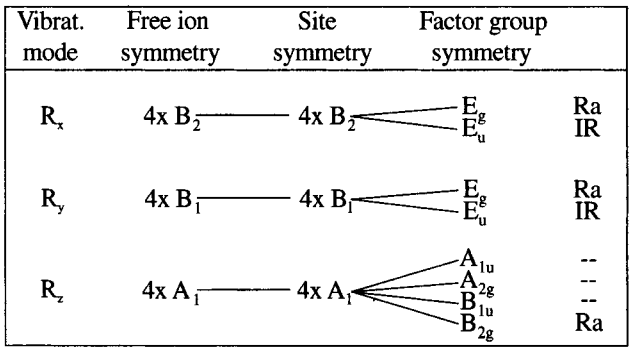

Figure 11. Correlation table for the normal librations of the amide ions in strontium and calcium amide (IR/Ra: expected to be observed in the infrared/Raman spectra).

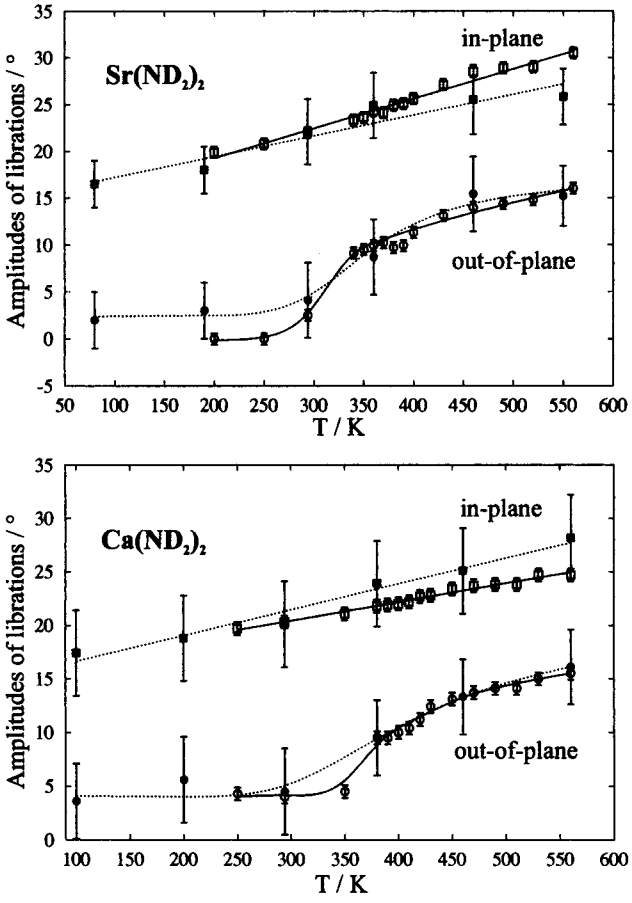

Figure 12. Temperature dependence of the amplitudes of the out-of-plane and the in-plane librations of the amide ions for both compounds. The open symbols denote results of the ^{2}H NMR experiments and the closed symbols are derived from recently published neutron diffraction measurements[12] (○: out-of-plane librations; ■: in-plane librations). The solid lines are a guide for the eyes for the ^{2}H NMR data and the dashed lines for the neutron scattering results.

than the one for $Sr(ND_2)_2$ (see Table 4) which may be because of the higher charge density of the calcium cations and the resulting smaller free volume for the amide ions. On the basis of a method of Biltz[49] who calculated volume increments for several ions from crystallographic data of ionic compounds, the free volume of an amide ion is 28.6 Å^3 for $Ca(ND_2)_2$ and 31.6 Å^3 for $Sr(ND_2)_2$, respectively.

The activation energy of the 180° jump process is larger for the calcium compound than for the strontium compound. On the basis of a simple electrostatic model, we estimated the reorientational potential using a program designed for the calculation of the Madelung part of the lattice energy (MAPLE) for different orientations of a central amide ion assuming that all other atoms remain fixed on their equilibrium positions.[8] On the basis of this ansatz we calculated the electrostatic activation energy using +2 and +0.3 for the partial charges of the metal cations and the deuterium atoms. The latter was estimated from the dipole moment of a free amide ion calculated by self-consistent field methods.[50] The calculated activation energies are 115.6 kJ/mol ($Ca(ND_2)_2$) and 94.0 kJ/mol ($Sr(ND_2)_2$), respectively. The absolute value is roughly twice that determined in the experiment, but the ratio between the values for $Ca(ND_2)_2$ and for $Sr(ND_2)_2$ is nearly the same (calculation = 1.229, experiment = 1.218). Keeping in mind the simplicity of our model this is a nice agreement which indicates that the reorientational potential is nearly electrostatic in nature.

The second dynamical process of the amide ion is a fast librational motion. We estimated values for the libration amplitudes from the quadrupole-coupling tensor obtained from the deuterium line shape analyses. Using a simple model (see previous section) we calculated characteristic values for the out-of-plane and the in-plane motion of the amide ions. Even at low temperatures, the amplitude of the in-plane libration is large and increases only slightly with rising temperature. In contrast, the amplitude of the out-of-plane librations are small at low temperatures but exhibit a strong increase at 304 K for $Sr(ND_2)_2$ and 368 K for $Ca(ND_2)_2$, respectively (see Figure 12). Its trend corresponds to the one found in neutron diffraction experiments.[12] Both temperature values agree well with the transition temperature of the anomalous effect of the thermal expansion. From this result it is highly plausible that both effects, namely the discrete change of the thermal expansion and the strong increasing of the out-of-plane libration amplitudes, are correlated.

Acknowledgment. Financial support of this work by the German Bundesministerium für Bildung, Wissenschaft, Forschung und Technologie under Contract 03-JA3DOR-6 and Contract 03-JA4DOR-3 is acknowledged.

References and Notes

(1) Juza, R. *Angew. Chem.* **1964**, *7*, 290.
(2) Juza, R.; Jacobs, H.; Klose, W. *Z. Anorg. Allg. Chem.* **1965**, *338*, 171.
(3) Juza, R.; Schumacher, H. *Z. Anorg. Allg. Chem.* **1963**, *324*, 278.
(4) Nagib, M.; Jacobs, H.; von Osten, E. *Atomkernenergie* **1977**, *29*, 41.
(5) Nagib, M.; Jacobs, H.; von Osten, E. *Atomkernenergie* **1983**, *43*, 47.
(6) Nagib, M.; Kistrup, H.; Jacobs, H. *Atomkernenergie* **1979**, *33*, 38.
(7) Müller, M. Dissertation, Universität Kiel 1996.
(8) Senker, J. Dissertation, Universität Dortmund 1996.
(9) Müller, M.; Asmussen, B.; Press, W.; Senker, J.; Jacobs, H.; Büttner, H.; Kockelmann, W.; Ibberson, R. M. *Physica B* **1997**, *234*−*236*, 45.
(10) Senker, J.; Müller, M.; Press, W.; Mayer, H. M.; Ibberson, R. M., Jacobs, H. *Physica B* **1997**, *234*−*236*, 51.
(11) Müller, M.; Senker, J.; Asmussen, B.; Press, W.; Jacobs, H.; Kockelmann, W.; Mayer, H. M.; Ibberson, R. M. *J. Chem. Phys.* **1997**, *107*, 2363.
(12) Senker, J.; Jacobs, H.; Müller, M.; Press, W.; Müller, P.; Mayer, H. M.; Ibberson, R. M. *J. Phys. Chem.* **1998**, *102*, 931.
(13) Müller, M.; Asmussen, B.; Press, W.; Senker, J.; Jacobs, H.; Büttner, H.; Schober, H. *J. Chem. Phys.* **1998**, *109*, 3559.
(14) Dufourc, J.; Chézeau, J. M.; Lemanceau *J. Mol. Struct.* **1996**, *4*, 15.
(15) Bouclier, P.; Portier, J.; Turrell, G.; Dufourc, J.; Hagenmuller, P. *C. R. Acad. Sci. Paris* **1969**, t. *268C*, 175.
(16) Hoaston, G. L.; Vold, R. L. ^{2}H NMR-Spectroscopy of Solids and Liquid Crystals; *NMR: Basic Principles and Progress*; Springer-Verlag: Berlin, 1994; Vol. 32.
(17) van Putten, D.; Diezemann, G.; Fujara, F.; Hartmann, K., Sillescu, H. *J. Chem. Phys.* **1992**, *96*, 1748.

(18) Hirschinger, J.; English, A. D. *J. Magn. Reson.* **1989**, *85*, 542.
(19) Siminovitch, D. J.; Ruocco, M. J.; Olejniczak, E. T.; Gutpa, S. K.; Griffin, R. G. *Chem. Phys. Lett.* **1985**, *119*, 251.
(20) Jeffrey, K. R. *Bull. Magn. Reson.* **1980**, *3*, 69.
(21) Wittebort, R. J.; Olejniczak, E. T.; Griffin, R. G. *J. Chem. Phys.* **1987**, *86*, 5411.
(22) Greenfield, M. S.; Ronemus, A. D.; Vold, R. L.; Vold, R. R.; Ellis, P. D.; Raidy T. E. *J. Magn. Reson.* **1987**, *72*, 89.
(23) Schadt, R. J.; Cain, E. J.; English, A. D. *J. Phys. Chem.* **1993**, *97*, 8387.
(24) Lin, T.; Vold, R. R. *J. Chem. Phys.* **1991**, *95*, 9034.
(25) Beckham, H. W.; Spiess, H. W. Two-Dimensional Exchange NMR Spectroscopy in Polymer Research; *NMR: Basic Principles and Progress*; Springer-Verlag: Berlin, 1994; Vol. 32.
(26) Schaefer, D.; Spiess, H. W. *J. Chem. Phys.* **1992**, *97*, 7944.
(27) Schmidt, C.; Blümich, B.; Spiess, H. W. *J. Magn. Reson.* **1988**, *79*, 296.
(28) Ta−Hsien, L.; Vold, R. R. *J. Magn. Reson.* **1995**, *A113*, 271.
(29) Müller, K.; Poupko, R.; Luz, Z. *J. Magn. Reson.* **1990**, *90*, 19.
(30) Spiess, H. W.; Sillescu, H. *J. Magn. Reson.* **1981**, *42*, 381.
(31) Abragam, A. *Principles of Nuclear Magnetism*; Oxford Science Publications: Oxford, 1961.
(32) Slichter, C. P. *Principles of Magnetic Resonance*; Springer-Verlag: Berlin, 1992.
(33) Brink, D. M.; Sachtler, G. R. *Angular momentum*; Oxford University Press: London, 1962.
(34) Spiess, H. W. Rotation of Molecules and Nuclear Spin Relaxation; *NMR: Basic Principles and Progress*; Springer-Verlag: Berlin, 1978; Vol. 15.
(35) Bloom, M.; Davis, J. H.; Valic, M. I. *Can. J. Phys.* **1980**, *58*, 1510.
(36) Spiess, H. W. *J. Chem. Phys.* **1980**, *72*, 6755.
(37) Barbara, T. M.; Greenfield, M. S.; Vold, R. L.; Vold, R. R. *J. Magn. Reson.* **1986**, *69*, 311.
(38) Jacobs, H.; Schmidt, D. *Curr. Top. Mater. Sci.* **1982**, *8*, 379.
(39) Davis, J. H.; Jeffrey, K. R.; Bloom, M.; Valic, M. I. *Chem. Phys. Lett.* **1976**, *42*, 390.
(40) Lin, T.-H.; Vold, R. R. *J. Magn. Reson.* **1995**, *A113*, 271.
(41) Heaton, N. J.; Vold, R. R.; Vold, R. L. *J. Magn. Reson.* **1988**, *77*, 572.
(42) Levitt, M. H.; Suter, D.; Ernst, R. R. *J. Chem. Phys.* **1984**, *80*, 3064.
(43) Kennedy, M. A.; Vold, R. R.; Vold, R. L. *J. Magn. Reson.* **1991**, *91*, 301.
(44) Heaton, N. J.; Vold, R. R.; Vold, R. L. *J. Am. Chem. Soc.* **1989**, *111*, 3211.
(45) Rabbani, S. R.; Edmonds, D. T.; Gosling, P. *J. Magn. Reson.* **1987**, *72*, 422.
(46) Laaksonen, A.; Wasylishen, R. E. *Z. Naturforsch.* **1995**, *50a*, 137.
(47) Hüttig, G. F. *Z. Anorg. Allg. Chem.* **1920**, *114*, 161.
(48) Rousseau, D. L.; Bauman, R. P.; Porto, S. P. S. *J. Raman Spectrosc.* **1981**, *10*, 253.
(49) Biltz, W. *Raumchemie fester Stoffe*; Verlag Leopold Voss: Leipzig, 1934.
(50) Lee, T. J.; Schaefer, H. F. *J. Chem. Phys.* **1985**, *83*, 1784.
(51) Schotte, U.; Schotte, K. D.; Kabs, M.; Dachs, H. J. Phys.: Condens. Matter **1992**, *4*, 9283.
(52) Schotte, U.; Schotte, K. D.; Bleif, H.-J.; Kabs, M.; Dachs, H. J. Phys.: *Condens. Matter* **1995**, *7*, 7453.